ISSN 1063-7729, Astronomy Reports, 2007, Vol. 51, No. 12, pp. 967–984. © Pleiades Publishing, Ltd., 2007.
Original Russian Text © E.E. Lekht, V.I. Slysh, V.V. Krasnov, 2007, published in Astronomicheskiĭ Zhurnal, 2007, Vol. 84, No. 12, pp. 1070–1088.

Variations in the Spectrum and Spatial Structure of the H_2O Maser in W75N

E. E. Lekht[1,2], V. I. Slysh[3], and V. V. Krasnov[4]

[1] *Instituto Nacional de Astrofísica, Óptica y Electrónica, Luis Enrique Erro No. 1, Apdo Postal 51 y 216, 72840 Tonantzintla, Puebla, México*

[2] *Sternberg Astronomical Institute, Universitetskiĭ prospekt 13, Moscow, 119991 Russia*

[3] *Astro Space Center of the Lebedev Institute of Physics, Russian Academy of Sciences, Profsoyuznaya ul. 84/32, Moscow, 117997 Russia*

[4] *Pushchino Radio Astronomy Observatory, Astro Space Center, Lebedev Institute of Physics, Russian Academy of Sciences, Pushchino, Moscow oblast', 142290 Russia*

Received March 12, 2007; in final form, June 22, 2007

Abstract—A probable model for the circumstellar envelope associated with the source VLA 2 in W75N has been constructed, based on H_2O-maser monitoring toward W75N carried out on the 22-m radio telescope in Pushchino, as well as VLA maps for 1992, 1996, 1998, and 1999. The envelope has a complex hierarchical structure, including individual maser spots, clusters and chains of spots, inhomogeneous filaments, individual arc-shaped layers, and other complicated features. Most widespread are multi-link chains or filaments with sizes of 1–2 AU. This pattern arises due to the complex hierarchical structure of turbulent motions of material on various scales, from microturbulence to large-scale chaotic motions. No expansion of individual layers in the envelope of VLA 2 has been found. The appearance of the layers is due to the passage of MHD waves that excite the maser emission in consecutive shells in the envelope. This process is fairly cyclic, and is related to the flare activity of the star.

PACS numbers : 97.10.Fy, 95.85.Bh
DOI: 10.1134/S1063772907120025

1. INTRODUCTION

The source W75N is associated with a region of active star formation and is located in the Cygnus X composite molecular complex at a distance of 2 kpc. Three ultracompact continuum sources (VLA 1, VLA 2, and VLA 3) and two clusters of maser spots have been detected in W75N, one associated with VLA 1, and the other with VLA 2 [1]. The continuum source VLA 1 extends 2000 AU northeast–southwest. VLA 1 is probably a radio jet or a disk hosting H_2O maser spots.

The other continuum source, VLA 2, is not spatially resolved. The H_2O maser spots here are clustered in two main zones arranged almost symmetrically about the central B star, which has a mass of $\approx 10\,M_\odot$. The system's radius is about 160 AU [2].

The pattern of maser spots in the sources and the evolution of their emission basically mirrors the morphology of various regions in the sources: Keplerian disks, bipolar outflows, and ultracompact HII regions with various configurations. Proper motions of maser spots are possible in all such configurations. For instance, Reid et al. [3] found a spatial displacement of H_2O maser spots in Sgr B2, which they suggest could be due to rotation and outflow of material from the source.

Based on long-term monitoring of water-vapor masers in regions of active star formation, it was found that circumstellar envelopes have a complex hierarchical structure with scales from several to several hundreds of astronomical units [4].

Using the high spatial resolution of the VLBA, Uscanga et al. [5] detected elongated structures consisting of maser spots with ordered velocities having lengths of about 2 AU, which they called "microstructures." These resemble strongly elongated open-ended ellipses and similar shapes. We will refer to such structures as multi-link chains or nonuniform filaments. Note that all of these are oriented nearly radially from the source. Uscanga et al. [5] suggest that such microstructures are due to turbulent motions and are short-lived, with lifetimes of several months.

Monitoring of the spectrum of the water-vapor maser in W75N has shown that the H_2O emission displays strong, mainly flare-like, variability, with the intervals between maxima being about 2–3 years [6].

The hydroxyl and methanol maser emission is concentrated in clusters, which tend to be associated with the ultracompact regions VLA 1 and VLA 2. The strongest OH maser spots are associated with VLA 1, and form an elongated arc with a velocity gradient, which can be described by a model with a rotating disk [7]. A strong flare of the OH maser emission was observed in 2000, which may have been a precursor of a stronger flare in 2003 with a flux density of 1000 Jy [8]. This OH maser flare was immediately preceded by a period of fairly high activity of the water-vapor maser [9].

2. OBSERVATIONS AND DATA PROCESSING

Monitoring of the W75N H_2O spectrum has been carried out on the 22-m radio telescope of the Pushchino Radio Astronomy Observatory since 1980. Results prior to 1998 have been published in several papers. Here, we consider new results of monitoring for 1999–2006, as well as monitoring data obtained in 1992–1998 [9, 10]. The antenna beamwidth at 22 GHz is 2.6′. The data obtained before 2005 were recorded using a 128-channel filter-bank spectrum analyzer with a spectral resolution of 7.5 kHz (0.101 km/s in radial velocity at 22 GHz), and after 2005 using a 2048-channel autocorrelator with a resolution of 6.5 kHz (0.088 km/s). The mean interval between successive observations was about 1.5 months. An antenna temperature of 1 K corresponds to a flux density of 25 Jy.

After converting the H_2O spectra to a radial velocity – flux density coordinate system, we made a catalog of the spectra. To characterized the activity of the central object by calculating the integrated flux and velocity centroid using the formulas

$$F_{\text{int}} = \sum_i F_i \Delta V_i$$

and

$$V_c = \sum_i F_i V_i \Delta V_i / \sum_i F_i \Delta V_i.$$

We distinguished individual components in the complex spectra using Gaussian fitting.

We obtained VLA maps of the H_2O masers using data from the open archive of the National Radio Astronomy Observatory (USA). The angular resolution was 80×105 and 71×94 mas. The spectral resolution of the 1992 and 1996 observations was 0.658 km/s, of the 1998 and 1999 observations 0.165 km/s, and the observations of June 23, 1999 0.082 km/s. The data reduction and map construction was carried out in the standard way using the NRAO AIPS software package. In view of the high signal-to-noise ratio of these data, we could apply super-resolution, which was a factor of five higher than the diffraction resolution, i.e., about 20 mas. In total, maps for five epochs from November 1992 to July 1999 were produced.

3. RESULTS

Figure 1 presents spectra obtained in 1999–2006 on the 22-m radio telescope of the Pushchino Radio Astronomy Observatory.

Figure 2a shows variations in the integrated H_2O flux (F_{int}) from 1992 to 2006. The vertical bars at the top mark epochs of minima, which divide the period 1992–2006 into separate time intervals. Flares of the hydroxyl maser emission occurred in the two intervals separated by the minimum at the end of 2000 [8]. Especially strong flares of the H_2O maser were also observed in these time intervals. The first was related to the maser activity in a broad V_{LSR} interval, and especially with two emission features at −2.5 and 4 km/s. The second flare was also associatedd with enhanced activity of the maser in a broad velocity interval and, in particular, with the emission at 10.5 and 13 km/s. The vertical bars (labeled T and Ep1–Ep4) at the bottom of the upper panel of the figure mark the three epochs of VLBA observations of Torrelles et al. [1] and the epoch of the VLA observations considered here, respectively. The time intervals with flares are labeled A–E (see Fig. 3 below). A smoothed curve of the variations in F_{int} for 1980–2006 is given in an insert.

Figure 2b shows variations in the velocity centroid calculated for two cases: the velocity interval from −9 to 17 km/s (solid curve) and the complete spectra (dashed curve). The radial velocities leading to these deviations of the centroid are given for the most prominent extrema. The dotted curve shows a fitted sine wave. When obtaining this curve, we took into account only the solid curve. The period of the sine wave is ∼13.5 years. This value is fairly consistent with the 11.5-year period derived from the minima of the integrated flux [10].

The important addition of the data after 1999 has unfortunately not enabled us to refine this period. The maser activity phase that began in 1997 continued in 2006, as well. According to the smoothed integrated flux curve (insert in Fig. 2a), there are two main intervals of maser activity and two secondary maxima, which are considerably weaker and precede the main phases of maser activity. The cyclic activity period found from the secondary maxima is about 11.5–12 years, and the period between the main maxima is longer than 12 years. There were also faster variations in the smoothed F_{int} curve with periods from

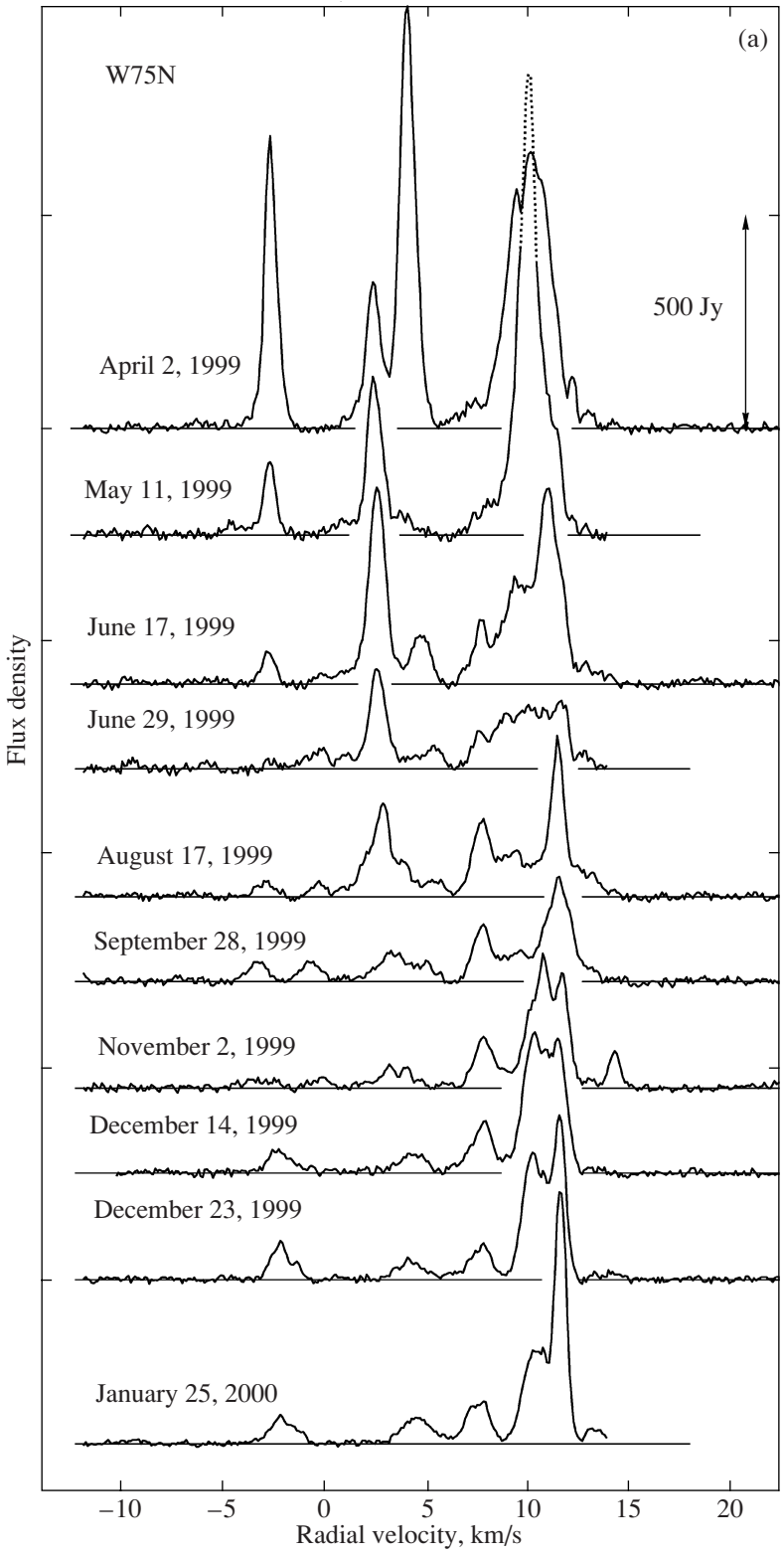

Fig. 1. H_2O maser spectra of W75N in 1999–2006. The double arrows show the scale in Janskys. The horizontal lines are the spectrum baselines.

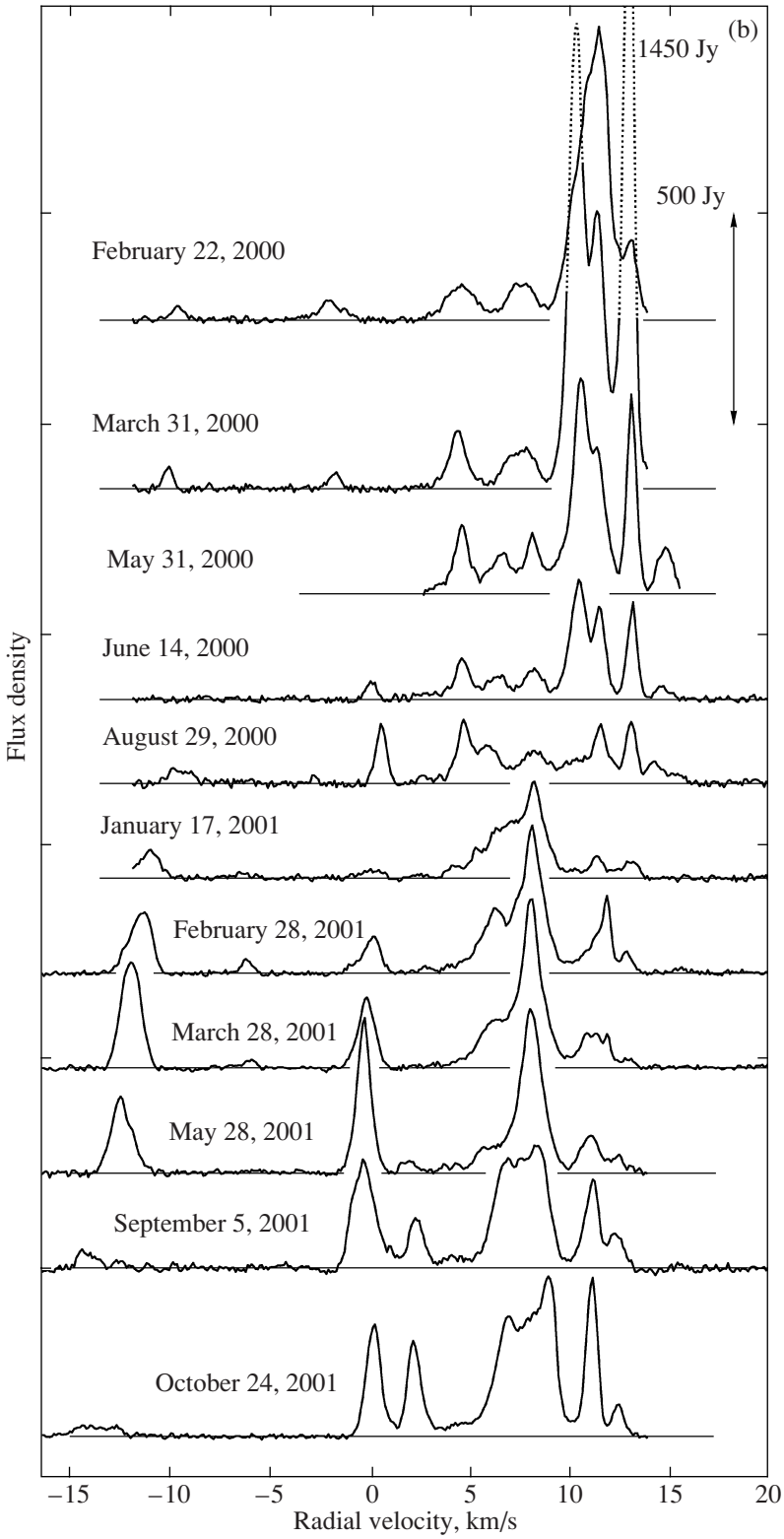

Fig. 1. (Contd.)

2.6 to 6.5 years, though individual strong bursts of the emission occurred more frequently, with a mean period of about 1.1 year.

The uncertainty in the period of the long-term variations in $F_{\rm int}$ is most likely due to the fact that, from time to time, the contribution of the emission

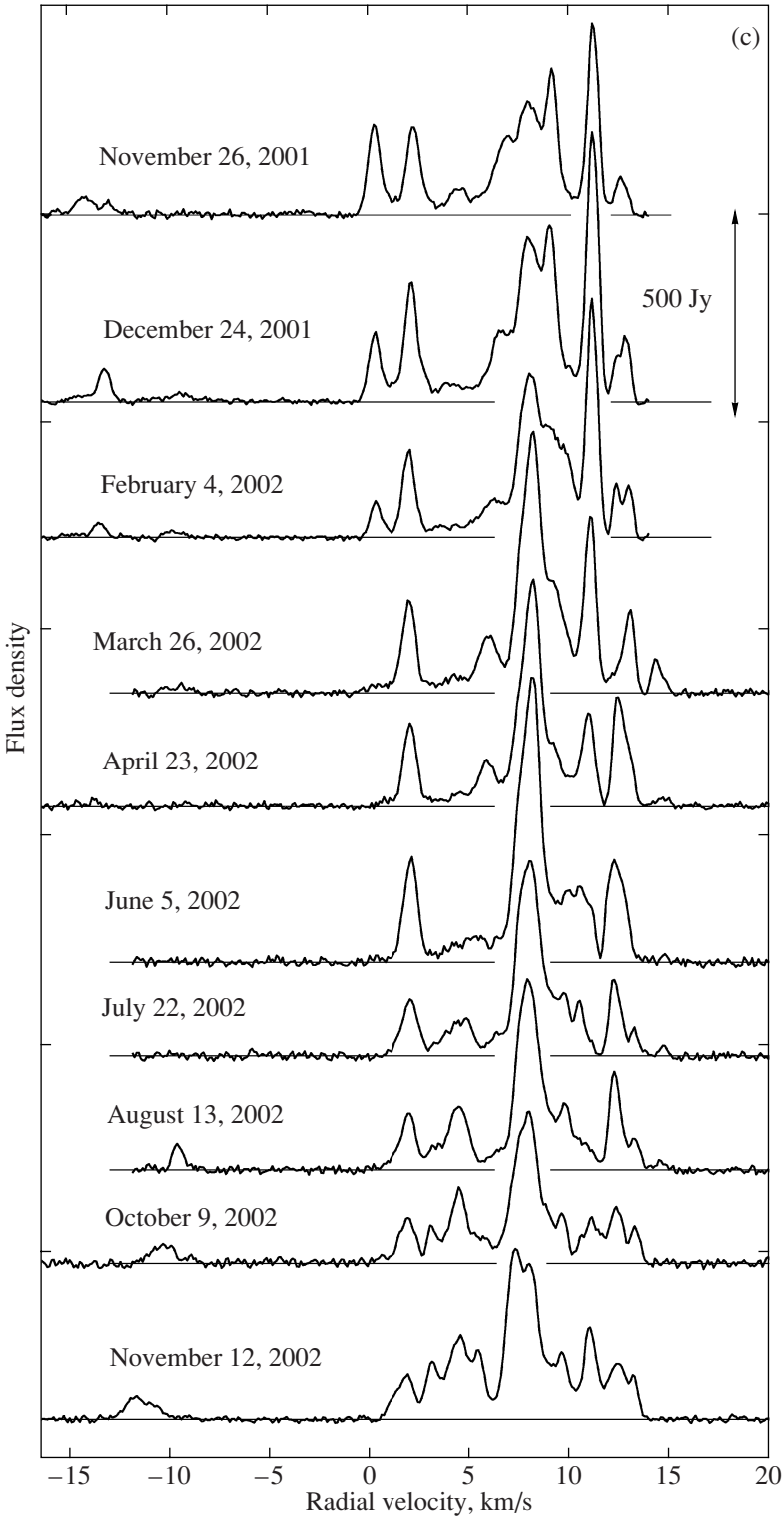

Fig. 1. (Contd.)

from VLA 1 to the total flux density can be important, and even dominate.

The emission variations at $V_{LSR} < -8$ km/s are unusual (Fig. 3), and appeared five times. We have denoted the individual components of this emission A, B, C, D, and E. In all cases, a strong radial-velocity drift was observed. The radial-velocity drift of each component is complex, and can be represented by

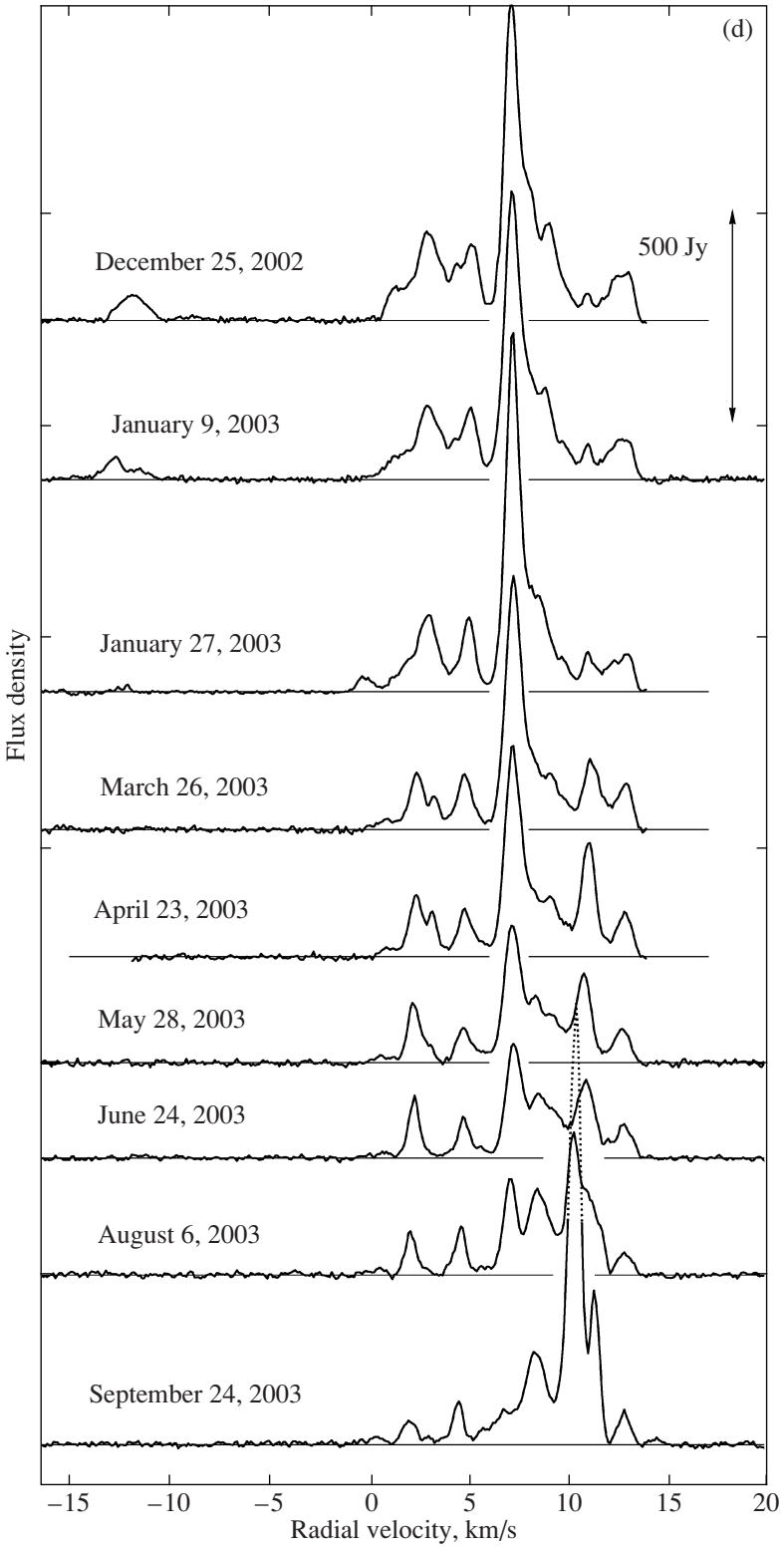

Fig. 1. (Contd.)

straight-line segments. In addition, there is a drift of the emission as a whole, shown by dashed lines. The observed evolution of the emission at velocities below − 8 km/s is probably associated with two flares, with this emission lagging in time the emission at velocities close to the cloud velocity. In case E, there are

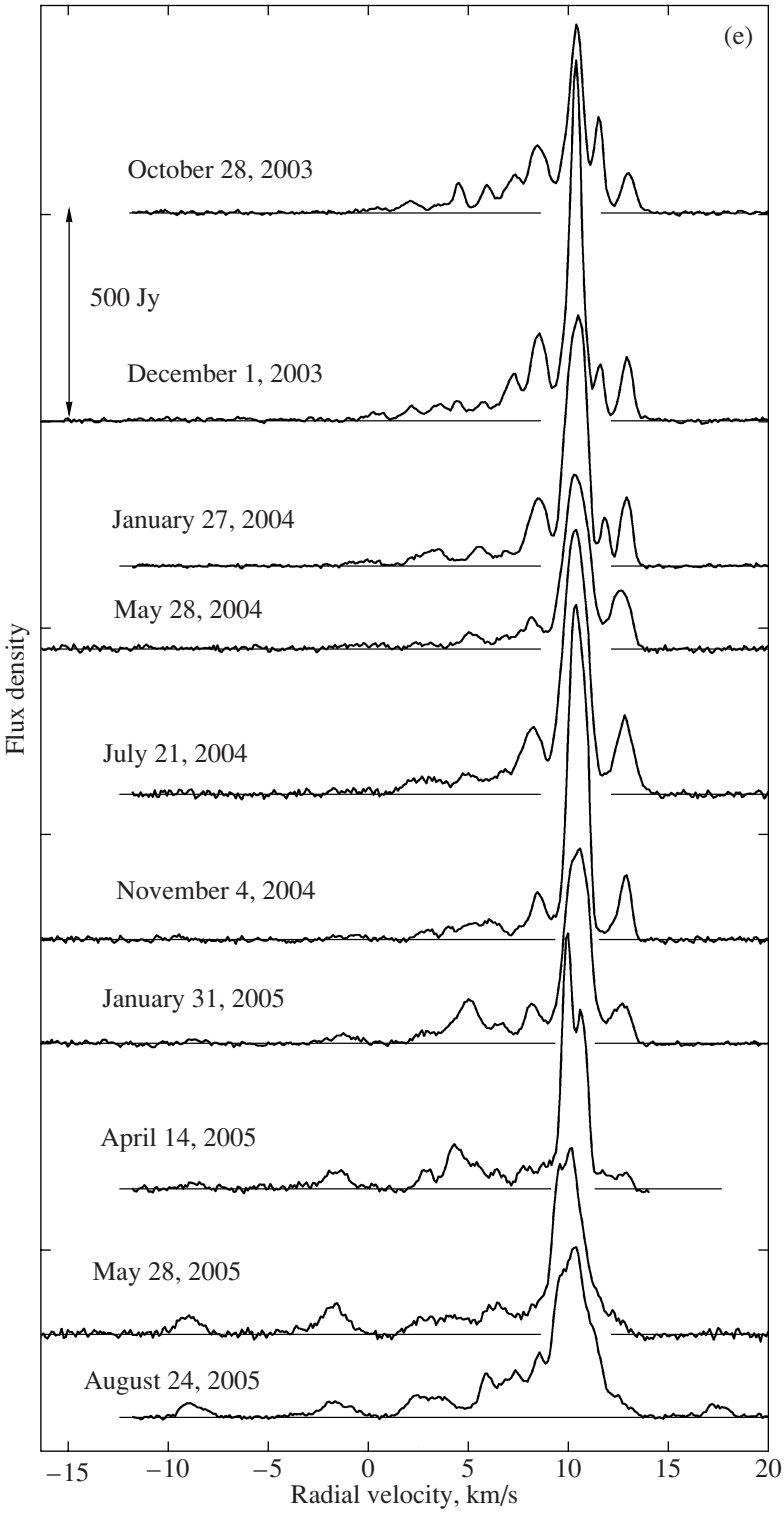

Fig. 1. (Contd.)

two emission features with drifts toward higher values of V_{LSR}.

Figure 4 shows the positions of the main maxima in the H_2O spectra from 1998 to 2005. We made no division into separate emission features. An exception was the period from the end of 2004 to mid-2006, when strong emission near 10 km/s with a complex structure was observed. For this period we divided the spectra into separate emission features; the main ones are plotted in Fig. 4.

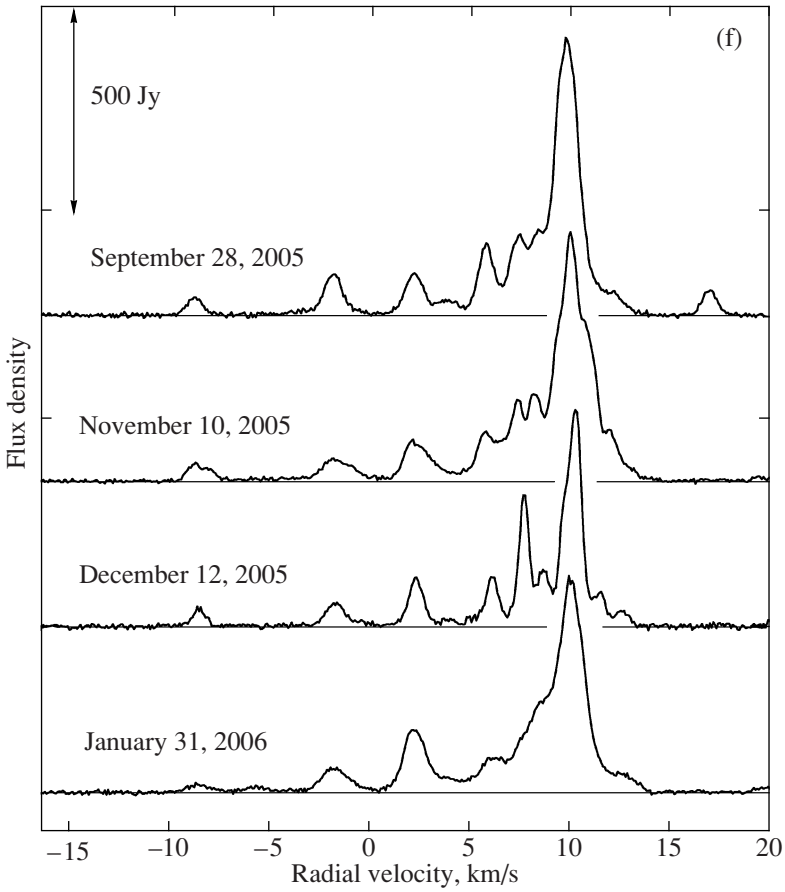

Fig. 1. (Contd.)

The maps for the five epochs of VLA observations are shown in Fig. 5 to the same scale. The coordinates are given relative to the point

$$\mathrm{RA}(1950) = 20^{\mathrm{h}}36^{\mathrm{m}}50.5^{\mathrm{s}},$$

$$\mathrm{Dec}(1950) = 42^{\circ}27'01.0''.$$

The large circles show the positions of VLA 1 and VLA 2. The position of the OH maser flare is shown by a large cross [11], whoses size corresponds to the position errors. On the 1999 map (Fig. 5d), the main zones of maser emission in VLA 2 are labeled I, II, III, and IV, and the triangle shows the position of a cluster of maser spots with $V_{\mathrm{LSR}} < -5$ km/s taken from [2].

Figures 6a and 6b show Zones I and III, respectively, where arc-shaped structures are most clearly visible. Using the (ΔRA, ΔDec) maps and dependences of V_{LSR} on ΔRA for each epoch, we have distinguished large-scale structures as well as groups (clusters) of maser spots and assigned them alphanumeric designations. The first three characters denote the observing epoch (from the first through fourth), and the remaining characters the mean clusters of spots at each epoch. The labels in brackets near some compact clusters of maser spots (Fig. 6b) are given when they can be identified with our monitoring data, according to the notation of Fig. 4.

The clusters of spots form ordered structures, that seem to correspond to chains having radial-velocity gradients. In most cases, the chains are arranged radially from the central object. A comparison of the maps for successive epochs separated by 1.3–4 years demonstrates discrepancies in the positions of separate groups of spots and of the arcs themselves. Even observations separated by one month display displacements of maser spots [2]. All this testifies to the presence of a very complex structure in the envelope surrounding the young star.

4. DISCUSSION

The W75N water-vapor maser is first of the sources included in our long-term monitoring project on the 22-m radio telescope in Pushchino for which we have analyzed our spectra jointly with VLA images for several epochs. This enables us to construct a model for VLA 1 and VLA 2, taking into account their evolution, and to estimate the character of the variability of protostars in these sources.

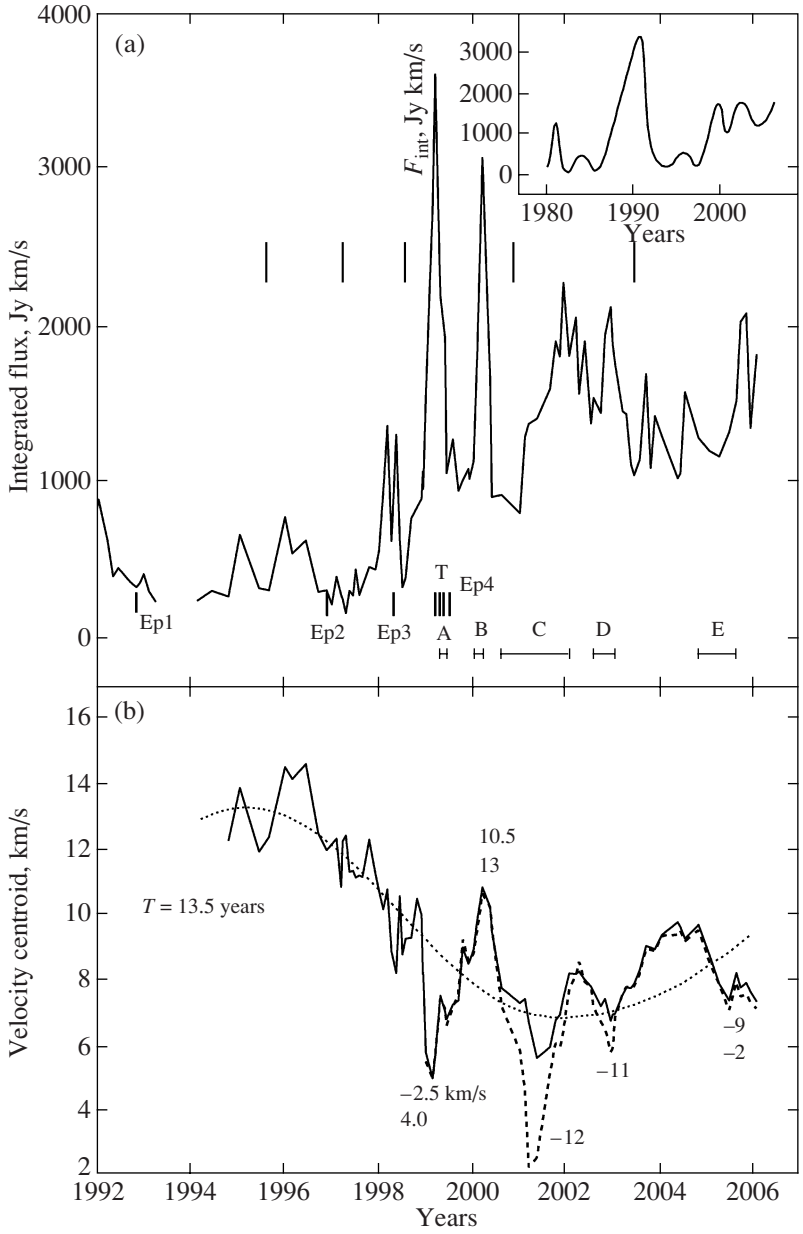

Fig. 2. Variations in the (a) integrated flux and (b) velocity centroid. The insert shows a smoothed curve of the variations of F_{int}. The vertical bars at the top of panel (a) show the epochs of minima, while those at the bottom sow epochs Ep1–Ep4 of the VLA observations (this paper) and epoch T of the VLBA observations of Torrelles et al. [2]. Intervals for some flares are labeled A through E. The dotted curve in panel (b) shows an approximation of the velocity centroid variation.

4.1. Velocities from −15 to −8 km/s

Maser emission at velocities from −15 to −8 km/s with flux densities exceeding 10–20 Jy was observed only rarely. During the strong flare of the entire maser in 1999–2000, we observed two successive short-lived flares in this region, which displayed strong drifts in V_{LSR} (A and B in Fig. 3). The strongest flares (C and D) took place in the next cycle of maser activity, in 2001–2003.

The emission in this V_{LSR} interval is most likely associated with VLA 2 for three reasons. First, according to Torrelles et al. [2], in 1999, the maser emission in VLA 2 was an order of magnitude stronger than the maser emission in VLA 1. Second, the maser emission of VLA 2 displayed a larger velocity dispersion that the maser emission of VLA 1. For this reason, maser emission at blueshifted velocities should belong to VLA 2. Third, the flares were correlated. This emission is most likely associated with Zone IV, where, according to Torrelles et al. [2], the maser spots have the greatest negative velocities and form a

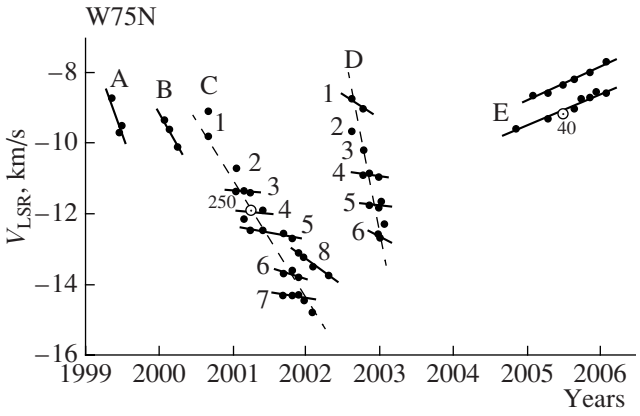

Fig. 3. Radial velocity variations of the emission features at $V_{LSR} < -8$ km/s. The drifts of individual features are approximated by straight line segments; clusters of features labeled with letters are shown with dotted lines.

very compact group elongated in the radial direction, with an extent of approximately 3–5 AU.

The composite character of the variations in components C and D (Fig. 3) can be explained by their elongated structure, e.g., having the form of chains formed by individual clumps of material. During a flare, a shock crosses each of these in succession, exciting emission. To estimate the extent of the chains, we adopt a shock velocity of about 10 km/s. Given the total time of activation of all elements in chains C and D (1.6 and 0.4 yr, respectively), the implied extent of the chains is 3.3 and 0.8 AU, consistent with the estimate of [2].

Also for comparison, we have determined the parameters of three elongated structures in the map of Torrelles et al. [2]. All the results are listed in the table. Components T_1, T_2, and T_3 are taken from the map of Torrelles et al. [2], T_3 for two epochs, May 7 and June 4, 1999 (denoted 3a and 3b). The radial-velocity gradient ΔV_{LSR} is reduced to a length of 1 pc.

We can see from the table that there is a good coincidence between the parameters of the elongated structures obtained in various ways: interferometric observations with high angular resolution and monitoring with high spectral and temporal resolution. The only difference is that they were observed at different epochs, and, therefore, in different cycles of flare activity of the maser. Note that single-dish monitoring can detect chains only during flares, when there is a radial-velocity gradient in the chains, and when there are sufficiently short time intervals between observations.

4.2. Comparison of the H_2O Monitoring Spectra with the VLA Maps

Here, we analyze all the data for 1992, 1996, and 1998–1999, when both the monitoring data and interferometric observations, including those of Torrelles et al. [2], are available.

Figure 7a presents a superposition of the spectra for 1988–1991, and Figs. 7b–7e superpositions of spectra that are close in time to the epochs of the VLA observations. The time intervals are shown. We have selected pairs of spectra: one before (dash–dot and dotted curves) and one after (bold curves) the VLA observations; the corresponding observation dates are given. For increased clarity, all the graphs (except for the upper one) are given on the same scale. The emission peaks identified with VLA 1 and VLA 2 are labeled with the source names. The vertical bars in Figs. 7d, 7e show the positions of the main components according to the VLA observations.

In 1992, the H_2O maser in VLA 2 was more active than the maser in VLA 1, while, in 1996, this situation is reversed. A comparison of the 1998 and 1999 maps with our monitoring data shows that the activity of the maser in VLA 2 became dominant. The minimum of its activity probably fell in 1994–1995.

Our identification shows that the emission at epoch 1 (1992) near velocities of 9 and 13 km/s is related to VLA 1. This implies that the strong flares observed in the monitoring of W75N in 1990 at 9.5 km/s and in 1989–1992 at 12.5 km/s [10] were associated with VLA 1.

Our monitoring indicates that the observations of Torrelles et al. [2] in 1999 fell in a period of high activity of the H_2O maser. This enables us to compare the results obtained using different methods, as we noted above.

We compared the three groups of features T_1–T_3 taken from the map of Torrelles et al. [2] with some components identified in our monitoring (Fig. 4 and the table). The radial velocities of individual features comprising components T_1–T_3 coincide with those for features revealed by the monitoring. This was especially clear in the case of component 10. The order of appearance of the emission features corresponds to

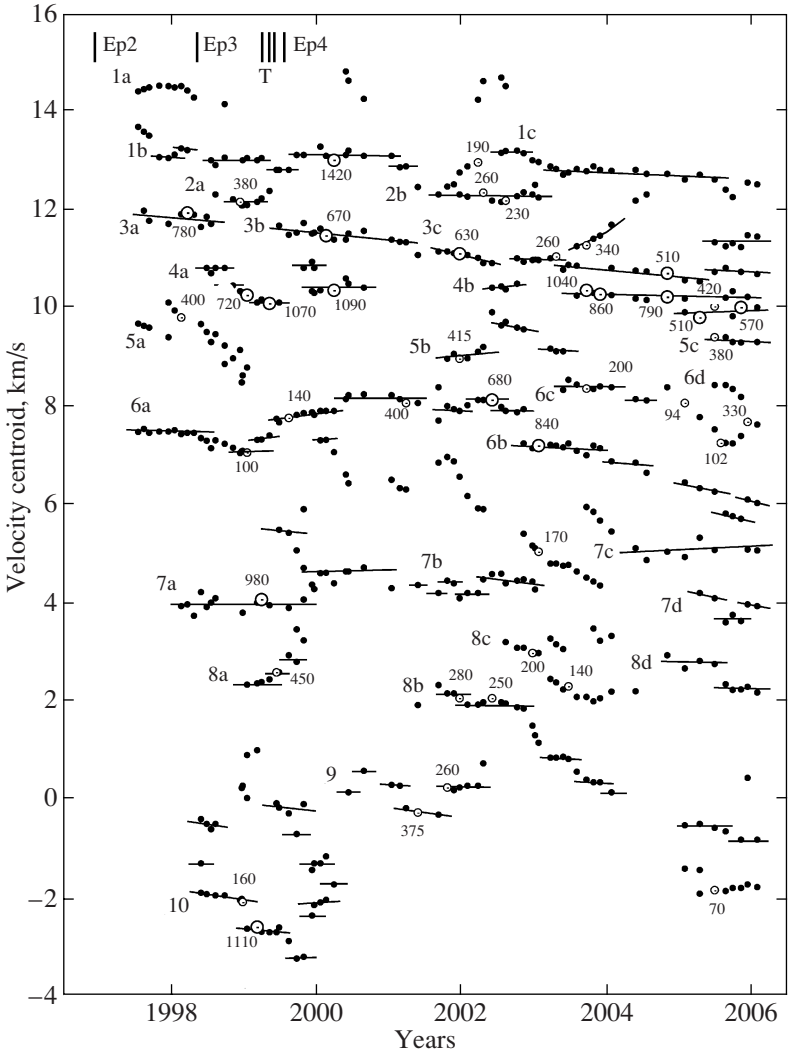

Fig. 4. Positional evolution of main emission peaks in the H_2O spectra. The horizontal segments connect points with similar velocities V_{LSR} (components). The small open circles with dots and large circles show the positions of emission peaks for local maxima with fluxes of 70–500 Jy and above 500 Jy, respectively. The labels indicate the flux densities in Jy. Most components (or groups) have alphanumeric designations. The vertical segments at the top mark the epochs of the VLBA observations of this work (Ep2–Ep4) and of Torrelles et al. [2] (T).

the order of their V_{LSR} arrangement in T_3 for May 7, 1999. However, one month later, the configuration of this group of features changed somewhat.

The general pattern of the variability in the structure of the H_2O spectra in 2004–2006 is complex. Time intervals of about two months between successive observations were not sufficiently short compared to the timescales for the evolution of individual emission features. In some cases, this resulted in a velocity scatter, and hindered assigning particular emission to some definite component.

The fast and strong variations in the spectra could be due to the composite structure of the envelope in VLA 2, which contains a large number of maser spots. The influence of the maser associated with VLA 1 was apparently low from 1992 to 2006. After 1992, the composite pattern of the variations in the W75N maser emission is mainly determined by the high and long-lived activity of the maser associated with VLA 2.

4.3. Analysis of the Maps and Identification

To increase our understanding of the evolution of the H_2O emission, we combined pairs of maps: epoch 1992 with 1996 and 1998 with 1999. An important justification for this is that the maser intensity was fairly low in 1992–1996, while the maser activity strongly increased in subsequent years.

4.3.1. Epochs 1992 and 1996. Hunter et al. [12] noted that the VLA observations toward W75N carried out on November 24, 1992 fell in a period of

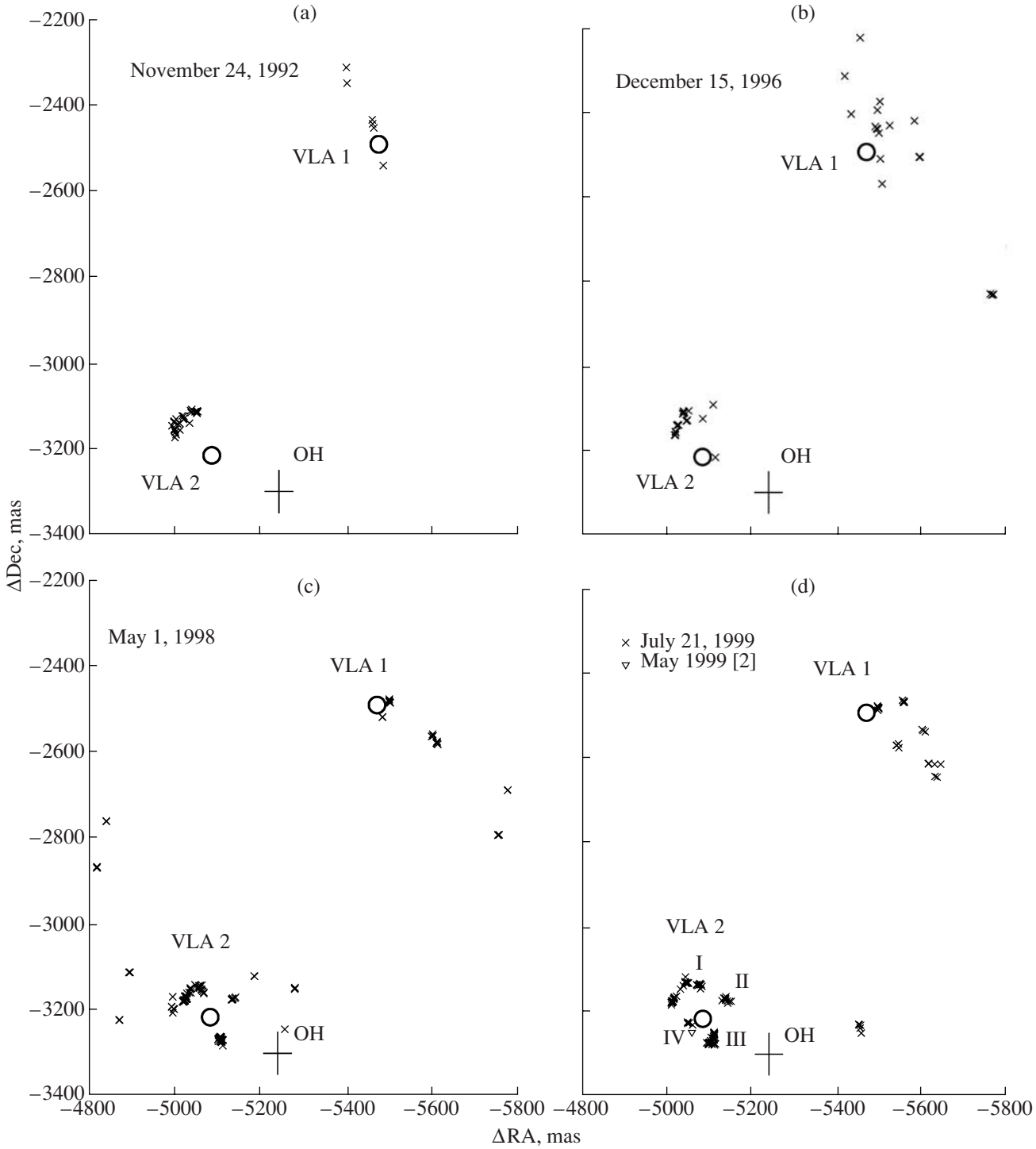

Fig. 5. Maps of the H_2O maser spots toward W75N at different epochs. The large circles show the positions of the continuum sources VLA 1 and VLA 2. The position of the strong flare of the OH maser is plotted with a large cross, showing also the measurement errors [11]. In the first of the two maps (epoch 1999) the main maser emission regions in VLA 2 are labeled I, II, III, and IV. A triangle shows the position of the cluster of maser spots with $V_{LSR} < -5$ km/s.

decline of the maser activity. The two main groups of maser spots in W75N are associated with VLA 1 and VLA 2. The highest integrated flux was from the maser in VLA 2.

At epoch 1992, the clusters of spots are mainly arranged along a single arc (Fig. 6a). It is quite possible that the cluster Ep1a, which is outside this arc, lies on another arc. In 1996, when the maser

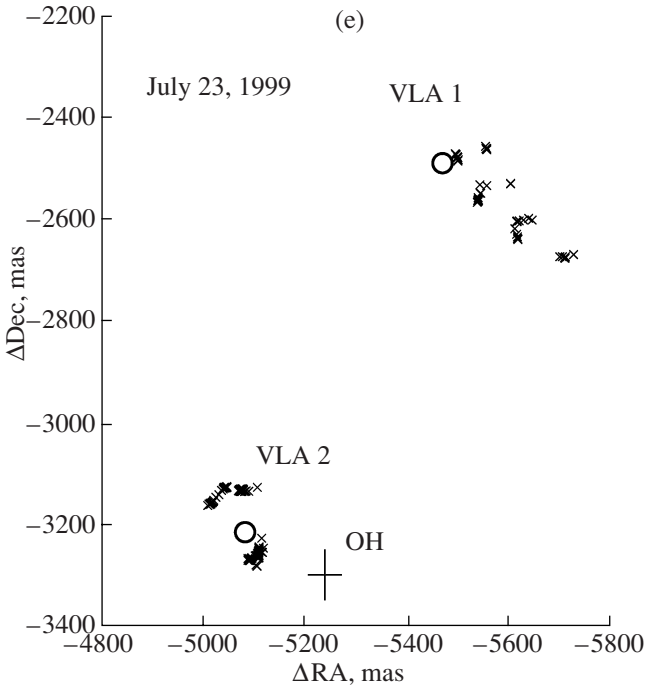

Fig. 5. (Contd.)

was at a still lower activity level, the maser spots were located closer to VLA 2, and are assembled in clusters, also forming an arc. A comparison of the maps for 1992 and 1996 demonstrates that the maser emission arises in different parts of the envelope.

4.3.2. Period 1998–1999. In this time interval, with high maser activity, emission in two new zones appeared in VLA 2 (Fig. 6b). Nevertheless, there was no complete envelope.

The clusters of spots observed in 1999 were located along an arc at a larger distance from the central star than the clusters observed at the preceding epoch, 1998 (Fig. 6a). However, Ep4a–Ep4c cannot be identified with Ep3b–Ep3d, and taken to be a consequence of expansion of the masing region from the central star.

With a mean distance between Ep3b–Ep3d and Ep4a–Ep4c of ∼10 mas (20 AU) and a time difference of ∼1.3 year, the velocity of the masing zone from the star should be appreciable, ∼75 km/s, which is considerably greater than obtained by Torrelles et al. (28 km/s). It is most likely that these clusters are different layers (arcs) in the zone of water-maser emission.

If we still suppose expansion, the lifetimes of the layers must be short, with these structures rapidly decaying and new ones continuously being born. In this case, in spite of the high probable velocity of motion of the layers relative to the central star (28 km/s), there would be no actual movement of the masing zone from the star. At first glance, precisely this situation follows from the VLA observations of 1992–1999.

Another masing zone (Zone II) has a more complex structure, observed only in periods of fairly high maser activity, in 1998 and 1999 (Fig. 6b). The maser spots observed in 1998 form a pattern that is similar to an opening spiral. The radial velocities of the spots are ordered in accordance with their positions on the map, and are identified with the monitoring components 1a, 3a, and 4a.

The configuration of the clusters of spots in 1999 includes elongated structures in which the radial velocities of the spots are ordered. The cluster Ep4h has the most complex structure, with the spot velocities displaying a close to sinusoidal behavior. This cluster is identified with two monitoring components, 3b and 4a (Fig. 4), with the main component being 4a. The powerful flares of 1998–2000 with peak flux densities above 1000 Jy are also associated with this component. Its evolution is best described by a chain of individual maser spots whose velocities decrease with distance from the star, from 11 to 10 km/s. This is consistent with the parameters of the cluster Ep4h.

5. A MODEL FOR VLA 2

Figure 8 presents a superposition of all the arcs approximating the pattern of maser-spot positions for Zone I of the maser emission, labeled with the dates of the corresponding observations. A multilayer structure of the envelope is visible. The layers observed

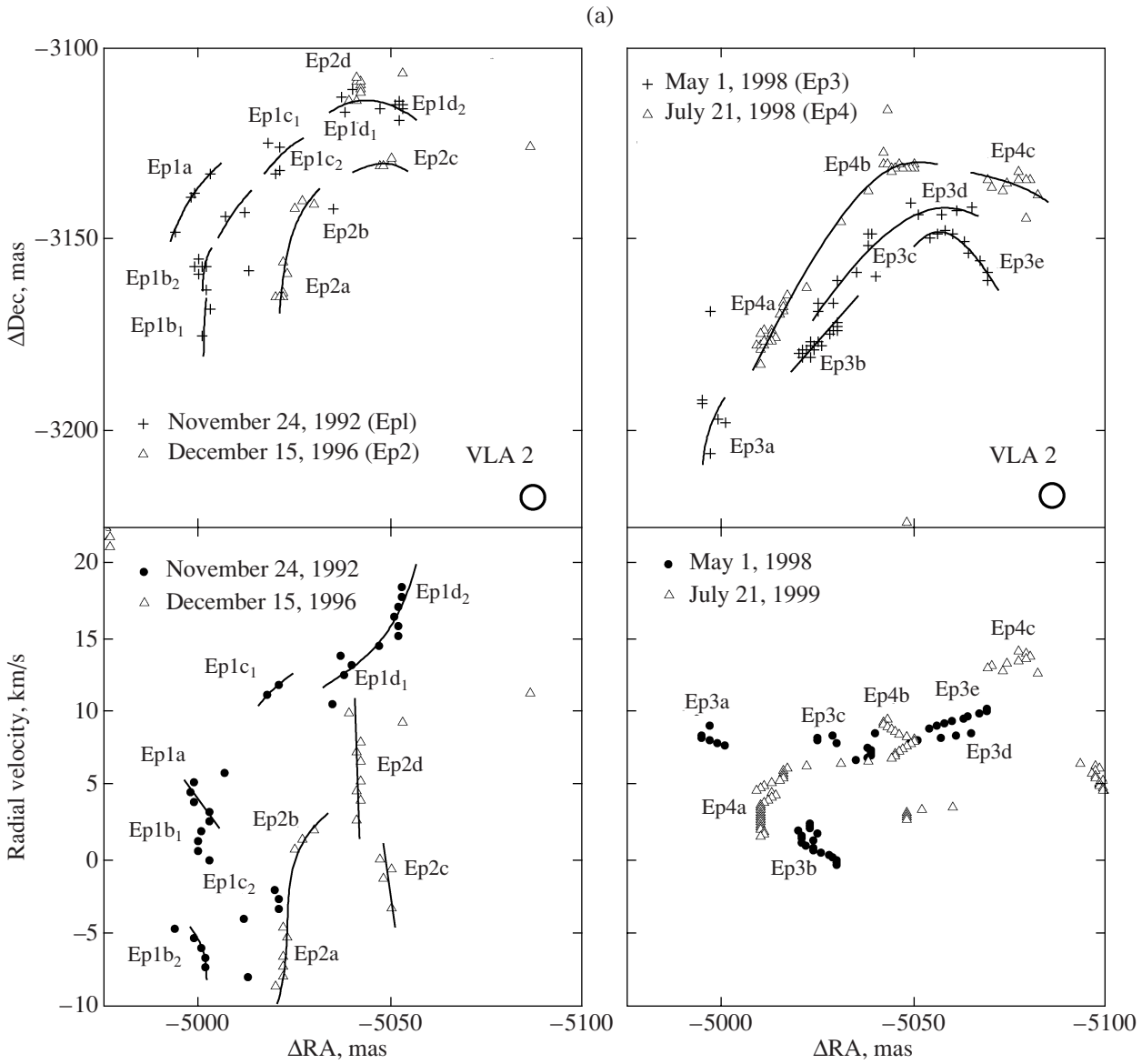

Fig. 6. (a) Zone I of the H_2O maser emission in VLA 2. The segments of curves delineate arc-shaped structures. Individual groups of maser spots are marked with alphanumeric labels. The first three characters indicate the epoch of the observations (from the first to the fourth), and the remaining characters the cluster number at each epoch. (b) Same as (a) for Regions II and III at epochs 1998 and 1999. The labels in parentheses for some clusters are given when they are identified with the monitoring data according to Fig. 4.

in 1996 and 1999 virtually coincide. The envelope in this masing zone probably has a relatively stationary multilayer structure, with shock waves crossing this structure (MHD waves) exciting the maser emission. Not all layers of the envelope are observed simultaneously, possibly due to fast de-excitation rather than an absence of continuous pumping.

As a model for the main cluster of maser spots Ep4h in Zone II, we propose that the maser spots and clusters of spots lie on an open ellipse. This structure is located in a plane perpendicular to the plane of the sky. As we can see from Fig. 6b, the middle of the ellipse is nearer to VLA 2 than its edges. There is a radial-velocity gradient along the ellipse: the near branch is approaches us, whereas the far branch is receding; i.e., it is as if the half-ellipse is in the process of straightening itself. The existence of such a structure is confirmed by the evolution of the spectrum, with jumps in V_{LSR} for the main spectral components. Such velocity jumps were continuously observed by us during our monitoring of W75N. As we already noted, they are due to the successive excitation of emission from elongated clusters of maser

(b)

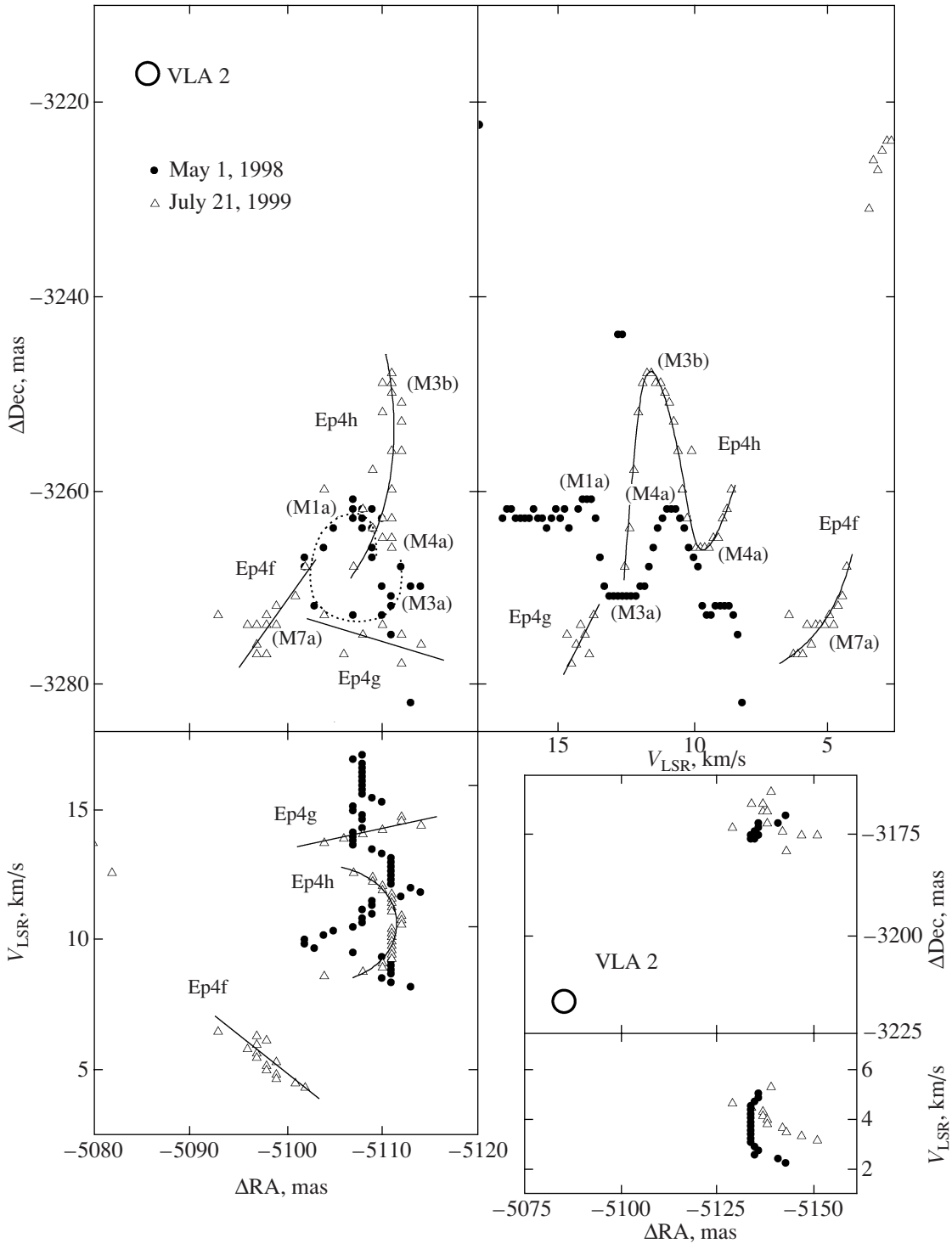

Fig. 6. (Contd.)

spots with radial-velocity gradients. The timescale for this phenomena ranges from ∼3 months to ∼1.5 year.

The difference in the configuration of Zone III in 1998 and 1999 could be due to differing levels of maser activity, as well as real changes in the "microstructures." According to our monitoring, two consecutive cycles of flare activity of the maser occurred in 1998 and 1999, with the maser being

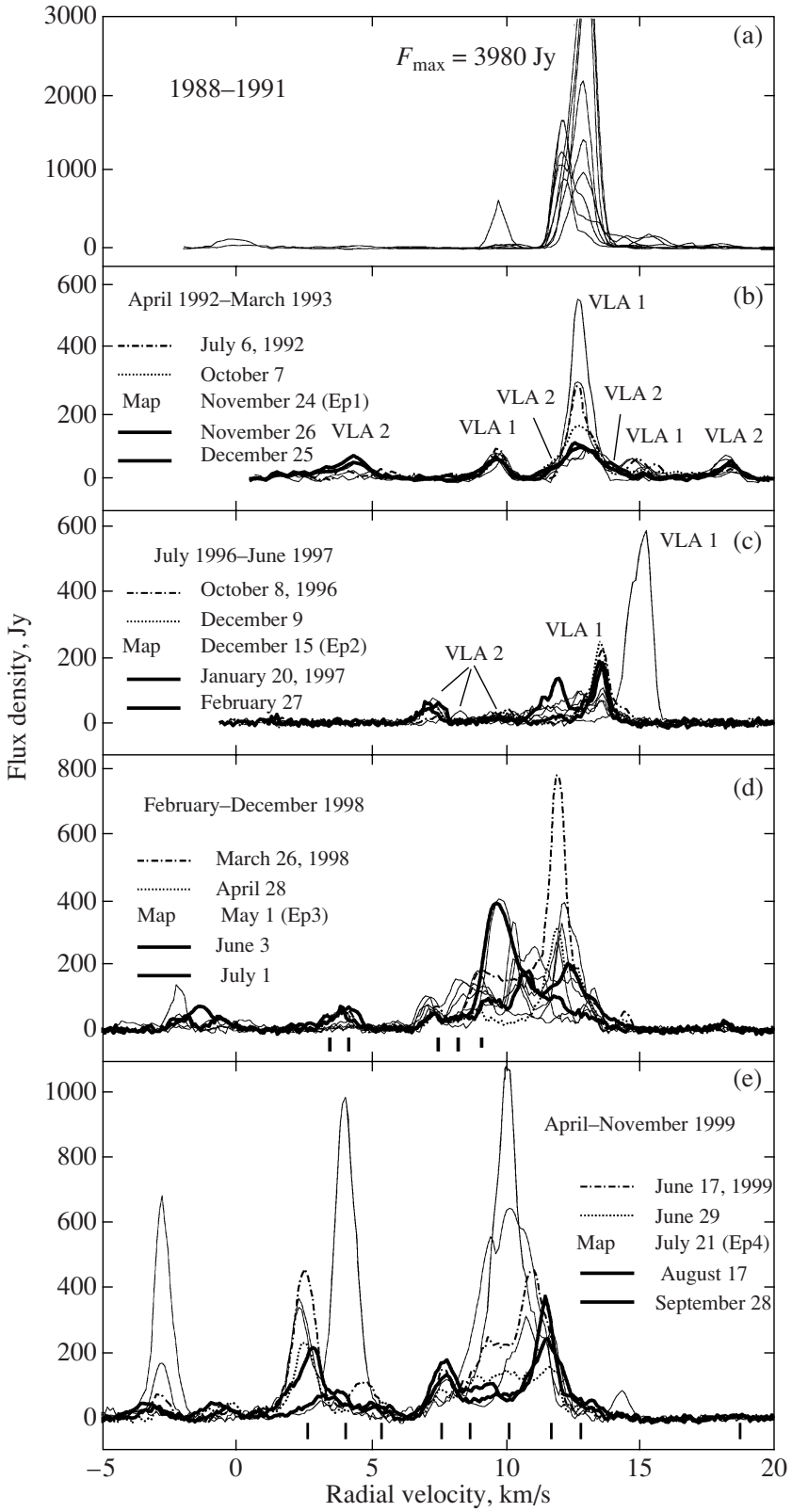

Fig. 7. Superposition of spectra close in time to the epochs of VLA-observations. Time intervals are shown. The dash-dotted, dashed and solid lines present the spectra near VLA-observations of each epoch. Segments of vertical lines on two lower plots show positions of basic components.

Parameters of individual H_2O components in W75N (VLA 2)

Component	Size, AU	Number of features	Mean step, AU	Interval of V_{LSR}, km/s		ΔV_{LSR} (km/s)/AU
T_1	0.5	4	0.17	10	11.7	3.4
T_2	1	7	0.17	5.4	7.9	2.5
T_{3a}	0.26	6	0.05	−3.5	− 1.4	8
T_{3b}	0.35	6	0.06	−3.5	− 1.4	6
C	3.3	8	0.47	−14.8	− 9.2	2
D	0.8	6	0.16	−12.8	− 8.5	5.3

more active in 1999. The composite structure of Zone III could be a consequence of turbulent motions of material in this part of the envelope, where real displacements of maser spots are also possible.

Thus, our studies of the evolution of the H_2O maser emission have shown that the envelope around the young star in VLA 2 has a composite hierarchical structure: there are individual maser spots, clusters of spots, chains or filaments, separate arc-shaped layers of the envelope, and other composite patterns. Such structures are clearly visible even in the monitoring data for the sources. This is due to the flare activity of the central star, whose mean period is estimated from the monitoring to be 1.1 year (Fig. 2a). An important condition for the detection of maser-spot chains is also the frequency of the monitoring observations. It is desirable to have intervals between successive observations no longer than one to two months. Otherwise, the observed character of changes in the radial velocities of emission features will inevitably result in misinterpretation, e.g., a simple drift of the maser spots owing to acceleration or deceleration.

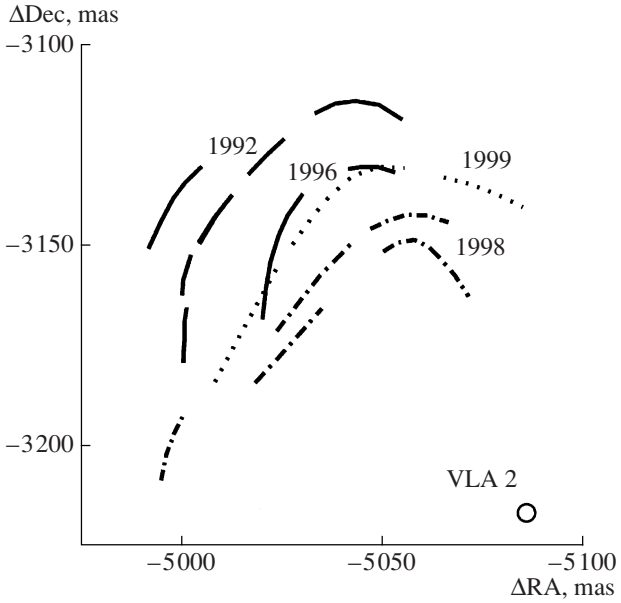

Fig. 8. Structure of the envelope in Zone I of the H_2O maser emission toward VLA 2 as observed with the VLA in 1992, 1996, 1998, and 1999.

6. CONCLUSIONS

Based on our monitoring of the W75N H_2O masers using the 22-m radio telescope of the Pushchino Radio Astronomy Observatory and VLA maps for 1992, 1996, 1998, and 1999, we have constructed a possible model for the circumstellar envelope associated with the source VLA 2 in the active star-forming region W75N. The envelope has a complex hierarchical structure, which includes individual maser spots, clusters and chains of spots, separate arc-shaped layers, and other composite features. Most widespread are multilink chains or nonuniform filaments with lengths of approximately one to two AU.

This structure arises from an intricate pattern of turbulent motions of material on various scales, from microturbulence to large-scale turbulence.

We have found no clear evidence of expansion of individual layers of the envelope in VLA 2. The appearance of these layers is due to the passage of MHD waves that excite maser emission in successive layers of the envelope. This process is more or less cyclic, and is associated with the flare activity of the star.

ACKNOWLEDGMENTS

The RT-22 radio telescope is supported by the Ministry of Education and Science of the Russian Federation (registration number 01-10). This work was supported by the Russian Foundation for Basic Research (project code 06-02-16806-a). The authors are grateful to the staff of the Pushchino Radio Astronomy Observatory for their help with the observations, and to the National Radio Astronomy Observatory (USA) for the VLA data from the open database.

REFERENCES

1. J. M. Torrelles, J. F. Gómes, L. F. Rodríges, et al., Astrophys. J. **489**, 744 (1997).
2. J. M. Torrelles, N. A. Patel, G. Anglada, et al., Astrophys. J. **598**, L115 (2003).
3. M. J. Reid, M. H. Schneps, J. M. Moran, et al., Astrophys. J. **330**, 809 (1988).
4. E. E. Lekht and N. A. Silant'ev, Izv. Ross. Akad. Nauk **67**, 335 (2003).
5. L. Uscanga, J. Canto, S. Curiel, et al., Astrophys. J. **634**, 468 (2005).
6. E. E. Lekht, Pis'ma Astron. Zh. **20**, 464 (1994) [Astron. Lett. **20**, 395 (1994)].
7. V. I. Slysh, V. Migenes, I. E. Val'tts, et al., Astrophys. J. **564**, 317 (2002).
8. A. V. Alakoz, V. I. Slysh, M. V. Popov, and I. E. Val'tts, Astron. Lett. **31**, 375 (2005).
9. E. E. Lekht and V. V. Krasnov, Pis'ma Astron. Zh. **26**, 45 (2000) [Astron. Lett. **26**, 38 (2000)].
10. E. E. Lekht, Astron. Zh. **72**, 31 (1995) [Astron. Rep. **39**, 27 (1995)].
11. V. I. Slysh and V. Migenes, Mon. Not. R. Astron. Sos. **369**, 1497 (2006).
12. T. R. Hunter, G. B. Taylor, M. Felli, and G. Tofani, Astron. Astrophys. **284**, 215 (1994).

Translated by G. Rudnitskii